

Artificial intelligence technique for estimating PV modules performance ratio under outdoor operating conditions

Alain K. Tossa,^{1,2} Y. M. Soro,^{2,a)} Y. Coulibaly,² Y. Azoumah,¹

Anne Migan-Dubois,³ L. Thiaw,⁴ and Claude Lishou⁴

¹KYA-Energy Group, 08BP 81101 Agoenyivé, Lomé, Togo

²LESEE-2iE, Laboratoire Energie Solaire et Economie d'Energie, Institut International d'Ingénierie de l'Eau et de l'Environnement, 01 BP 594 Ouagadougou 01, Burkina Faso

³GeePs—Laboratoire Génie électrique et électronique de Paris, 11, rue Joliot Curie, Plateau de Moulon, 91192 Gif sur Yvette Cedex, France

⁴Ecole Supérieure Polytechnique de Dakar, Corniche Ouest BP: 5085 Dakar-Fann, Senegal

(Received 30 May 2018; accepted 3 October 2018; published online 23 October 2018)

In this paper, artificial neural networks (ANNs) have been used for the performance ratio modelling of four photovoltaic (PV) modules. The PV modules are selected from three different silicon technologies including one monocrystalline, two polycrystalline, and one micromorph (a-Si/ μ c-Si) modules. The adopted ANN architecture is a multilayer perceptron (MLP). The inputs of the ANN models are the solar irradiance on the PV module plane and air ambient temperature, while the output is the PV module performance ratio. It is shown that ANN models with three layers and five hidden neurons accurately model the performance ratio regardless of PV module technology. The results obtained from the ANN model are compared with those obtained from the five parameter model (L5P). The model comparison is done through two widely used forecasting errors: the root mean square error (RMSE) and the mean absolute percentage of error (MAPE). The values of both RMSE and MAPE are less than 0.02 for MLP based models and are about three to nine times lower than those obtained from the electrical model. It is also shown that the poor fit of the L5P model is due to the bad estimation of series and shunt resistances. *Published by AIP Publishing.* <https://doi.org/10.1063/1.5042217>

I. INTRODUCTION

The use of photovoltaic modules, for electricity generation purposes, has seen greatest improvement in the world, in recent decades. In 2012, the total capacity of PV installed in the world reached 100GWp milestone, with 30.5 GWp installed that year. This capacity was about 227 GWp at the end of 2015 ([World Nuclear Association, 2017](#)). In the World Energy Outlook 2016 New Policies scenario, 1405 GWp of solar PV capacity would be operational in 2040, producing 2137 TWh/year.

On the other hand, there are different technologies of photovoltaic modules in the market. Their characteristics measured in standard test conditions (STCs) and provided by manufacturers are, however, rarely reached in real operating conditions. In fact, the performances and ageing of PV modules strongly depend not only on the technology but also on both the climatic and the environmental conditions of the installation site.

Several studies focused on the determination, for a given environment, of the photovoltaic technology that provides the best trade-off between the cost and PV module performances. These studies show that the performances of a PV module under real conditions depend on the weather ([Amrouche *et al.*, 2013](#); [Makrides *et al.*, 2009](#); and [Merten *et al.*, 2008](#)), the solar

^{a)}Author to whom correspondence should be addressed: moussa.soro@2ied-edu.org. Tel.: (+226) 68 76 88 22. Fax: (+226) 25 49 28 01.

spectrum, the spectral response of each technology (Cañete *et al.*, 2014), the module/cell design (Bücher, 1997), and the atmospheric conditions (dust and dirt) (Almonacid *et al.*, 2011).

At this level, an important question arises: which parameter can be used to evaluate the gap between the STC power and the real power (for a given site), which depend on both the technology and the site environment?

Consequently, many scientists have developed several metrics with different levels of complexities. Among them, the most used one is the performance ratio (PR) (Phinikarides *et al.*, 2014; Sharma *et al.*, 2013) which is recommended by the standard IEC 61724 for the assessment of PV systems (Merten *et al.*, 2008; Merten *et al.*, 2009) or PV module performances in a real environment (Cornaro and Musella, 2011; Tossa *et al.*, 2016). The PR can be used to compare different PV technologies in order to choose the best one for a specific climate zone (Aste *et al.*, 2014; Sharma *et al.*, 2013; Tossa *et al.*, 2016). The PR is also helpful to compare PV modules with different STC powers since it normalizes the energy produced under real conditions (in a time interval) to the maximum power at STC and to the incident solar radiation.

One of the biggest challenges faced in calculating the PR is the recording of the PV module characteristics under actual operating conditions. This process however implies an experimental set-up and a waiting time of months or even years to obtain relevant data that can be accurately analyzed. This method is time consuming and also needs expensive investment in the experimental set-up.

How can the PV module performance ratio be estimated accurately, faster, and at lower cost? To deal with the above-mentioned question, in this paper, the modeling of the electrical behavior of PV modules will be performed in order to estimate their performances, once the weather data of any given climate zone are available.

Different solar cell models have been developed to describe the PV module behavior, but the electrical equivalent circuit is a convenient and common way used in many studies (Bonkoungou *et al.*, 2013). An overview of various commonly used electrical equivalent circuit models has been presented in a previous work (Tossa *et al.*, 2014). The results of these previous studies showed that the use of electrical models is subject to two difficulties. First, they are characterized by electrical parameters linked by implicit and non-linear equations that are often very difficult to be solved. Second, they do not always enable the direct determination of the desired performance indicators, while intermediate calculations introduce inaccuracies.

To overcome these difficulties, Artificial Neural Networks (ANNs) are now increasingly used to model the electrical characteristics of photovoltaic modules. The modelled characteristic can be the output power (Almonacid *et al.*, 2014; Mellit *et al.*, 2013; Velilla *et al.*, 2014), the operating current (Celik, 2011; Karamirad *et al.*, 2013), the module temperature (Ceylan *et al.*, 2014b, 2014a), etc. All these studies systematically consider the solar irradiance and the ambient temperature as the ANN inputs. Some studies (Celik, 2011; Karamirad *et al.*, 2013; and Velilla *et al.*, 2014) consider additional input parameters such as the ambient humidity and the operating voltage, depending on the predicted parameter. After designing the ANN, the authors usually compare their outputs with the measurements and sometimes with the conventional electrical model outputs. They generally find that the ANN models outperform the electrical models, but there are very few studies which deeply bring out the weaknesses of electrical models in their current stage of development.

Moreover, the use of ANN models for the estimation of the PV module performance ratio as a function of the solar irradiance and the ambient temperature is not common in the literature.

The main objective of this paper is to develop a simple and accurate ANN-model taking into account the solar irradiance and the ambient temperature in order to estimate the real outdoor performance ratio of different PV module technologies. To assess the performance of the ANN models developed, a comparison of their results and those obtained with one-diode and five parameter (L5P) models will be carried out.

This paper consists of 4 sections including this one. Section II provides a description of the experimental PV test facility. The assessment of the module performance ratio, from both electrical and ANN-based models, is presented in Sec. III. Finally, results and discussion are presented in the last section.

II. MODULE TEST FACILITY

The current study is performed on four silicon photovoltaic modules of three different technologies: monocrystalline (mono-Si), polycrystalline (pc-Si), and amorphous tandem structure, also called micromorph (a-Si/ μ c-Si). Two pc-Si PV modules from different manufacturers (A and B) are considered. The four PV modules are labeled VIC003, VIC006, SUN011, and SHA017. Table I presents their STC characteristics as provided by the manufacturers.

The PV modules are characterized with a test facility named “I-V bench” from April 1, 2015 to July 13, 2015 (about 3.5 months). Figure 1 shows (a) the schematic diagram of the I-V curve measurement and (b) the outdoor installed PV modules and the meteorological measurement equipment of the I-V bench. This test facility is installed on the experimental platform of the Laboratory of Solar Energy and Energy Savings ($12^{\circ}26'48''$ North, $1^{\circ}33'45''$ West) nearby Ouagadougou (Burkina Faso) and entirely dedicated to the outdoor characterization and the monitoring of PV modules’ performances.

The PV modules are oriented southwards and tilted at an angle of 14° , close to the latitude ($12^{\circ}26'48''$ North) of the site. Some onsite experiments recommend the inclination angles to be slightly superior to the latitude (14° or 15°) to favor self-cleaning of dust and water streaming. The height of the roof is 3.15 m, and the distance between the PV modules’ bottom and the roof is around 1 m, favorable for good air circulation under the PV modules.

The I-V bench regularly measures the I-V characteristics, the temperature of each connected PV module, as well as the atmospheric conditions (solar irradiance, ambient temperature, relative humidity, wind direction and velocity, etc.). This methodology has been used by different research teams for photovoltaic module characterization (Cañete *et al.*, 2014; Kurnik *et al.*, 2011; Makrides *et al.*, 2008; Mosalam Shaltout *et al.*, 2000; Ndiaye *et al.*, 2014; Piliougue *et al.*, 2011; Rüther *et al.*, 2002; and Sharma *et al.*, 2013). The time interval between data measurements of two I-V curves is set to 5 min. The required time for a complete I-V curve record is short enough (less than 2 s) so that the solar irradiance can be considered constant for all the points. For each curve, the open circuit voltage according to the actual weather is first measured. Then, the voltage scanning is done from -0.5 V to 105% of V_{oc} . The voltage scanning is performed through an automatic variable load (Kepco Bop Power Supply) shown in Fig. 1. The desired number of points for the I-V curve plot can also be set (100 points are generally sufficient). For each point, three multimeters measure simultaneously the module voltage, the module current, and the solar irradiance. PV module I-V data are measured in a four-wire configuration in order to avoid errors due to voltage drop.

The module temperature is measured at the back of the module thanks to a Pt100 temperature sensor stuck on a solar cell at the center of the module. The Pt100 temperature sensor is fixed with a thin aluminium tape to avoid the modification of the conductive thermal flows within the module as mentioned by other authors (Guérin de Montgareuil *et al.*, 2009;

TABLE I. Electrical characteristics (STC) of the studied PV modules.

PV Module (Technology/name/manufacturer)				
	Mono-Si/VIC003/A	pc-Si/VIC006/A	pc-Si/SUN011/B	aSi:H/ μ c-Si:H/SHA017/C
I_{sc} (A)	3.16	3.09	2.95	3.45
V_{oc} (V)	22.2	22.2	22.1	59.8
I_{mp} (A)	2.78	2.85	2.75	2.82
V_{mp} (V)	18	18	18.2	45.4
P_{mp} (Wp)	50	50	50	128
I_{sc} temperature coefficient ($^{\circ}\text{C}$)	+0.037	+0.05	+0.081	+0.07
V_{oc} temperature coefficient ($^{\circ}\text{C}$)	-0.34	-0.35	-0.37	-0.30
P_{mp} temperature coefficient ($^{\circ}\text{C}$)	-0.48	-0.47	-0.45	-0.24
Area (m^2)	0.4104	0.4087	0.4624	1.4217
Efficiency	12.18%	12.23%	10.81%	9%

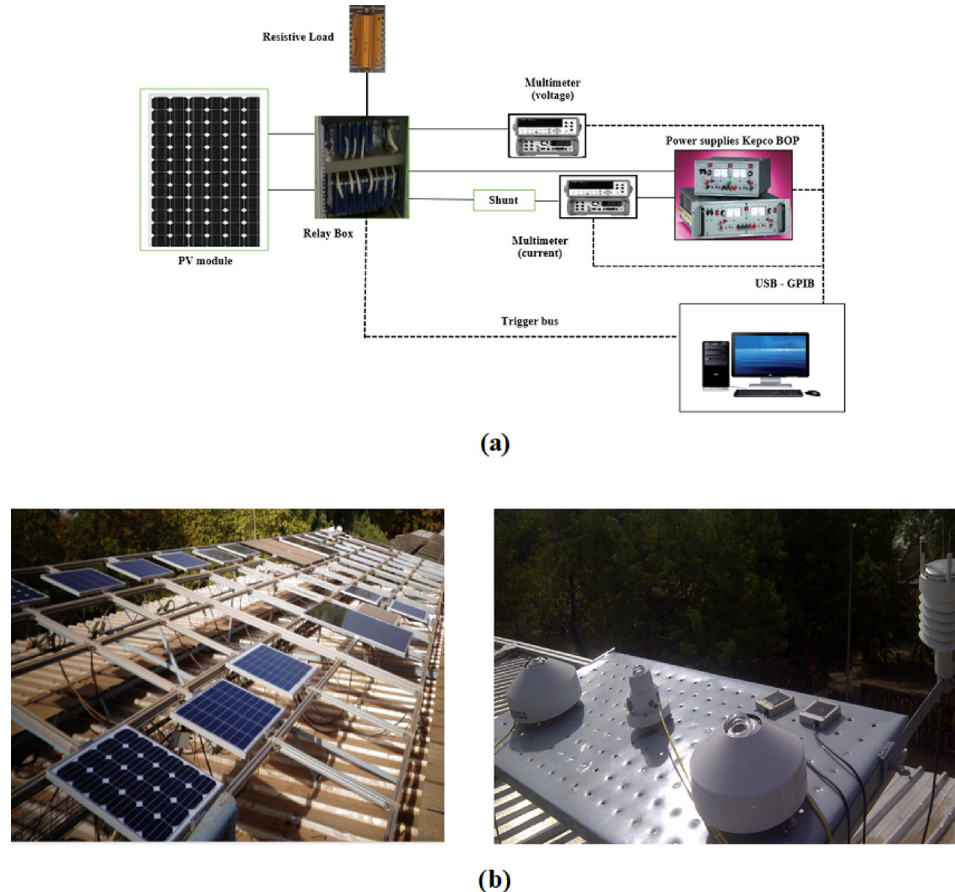


FIG. 1. I-V bench. (a) The schematic diagram of the I-V bench; (b) Modules installed outdoor and meteorological measurement equipment.

[Sicot et al., 2013](#)). When the I-V measurement of the first PV module (that takes less than 2 s) is going on, the others are connected to their resistive load [see Fig. 1(a)]. This PV module is then disconnected from the set-up and connected to its resistive load, while the next PV module is immediately connected to the set-up for its characterization. Once the four PV modules have been characterized, the process restarts after a five-minute rest. Thus, there are around five minutes between consecutive curves of a given PV module. The measurement devices were chosen to enable the collection of I-V data even at a very low irradiance around 0 W/m^2 . The I-V characteristic data are then systematically organized, classified, and stored in a CSV format file together with the corresponding time, working conditions (sun radiation intensity, ambient temperature, and wind speed), and the modules' temperatures.

The specifications of the main measurement devices as well as their accuracy are listed in Table II. The accuracies of the devices generally depend on the values of the measured quantities. [Piliougine et al. \(2011\)](#) have developed certain formulas to access the absolute uncertainty when the value of the measured quantity is known.

III. METHOD OF PERFORMANCE RATIO (PR) CALCULATION

A. PR calculation from outdoor measurements

The performance ratio (PR) measures the deviation between the actual efficiency (η) of a PV module and that is theoretically achievable (η_{STC}) under standard test conditions (STCs) ([Aste et al., 2014](#)). The PR is defined by the following equation(IEC 61724):

TABLE II. Specifications of the I-V bench measurement devices and accuracies.

Measurement devices and model	Measured parameter	Absolute uncertainty (Kamkird <i>et al.</i>, 2012 and Piliougue <i>et al.</i>, 2011)
Multimeter Agilent 34410A	DC voltage (V)	$\Delta U = 2\sqrt{7,1 \times 10^{-10} \cdot V^2 + 1,4 \times 10^{-7} \cdot V + 6,8 \times 10^{-6}}$
Multimeter Agilent 34410A	DC current (A)	$\Delta I = 2\sqrt{8,6 \times 10^{-6} \cdot I^2 + 8,9 \times 10^{-8} \cdot I + 1,8 \times 10^{-6}}$
Pyranometer CM11 Kipp & Zonen	Irradiance (W/m ²)	$\pm 3\%$ of the measured quantity.
Pt100 sensor class B	Module temperature (°C)	$\Delta T_{mod} = 2 \cdot \sqrt{8,3 \cdot 10^{-6} \cdot T_{mod}^2 + 10^{-3} \cdot T_{mod} + 4,6 \cdot 10^{-1}}$

$$PR = \frac{\eta}{\eta_{STC}}, \quad (1)$$

where the subscript STC refers to standard test conditions. The efficiencies η and η_{STC} are defined by Eqs. (2) and (3), respectively,

$$\eta = \frac{P_{mp}}{G*A}, \quad (2)$$

$$\eta_{STC} = \frac{P_{mp,stc}}{G_{STC}*A}, \quad (3)$$

where A and P_{mp} are the surface and the maximal power of the considered module, respectively. G is the solar irradiance.

The performance ratio is deduced from the outdoor measurements through three steps. First of all, the recorded I-V data are filtered to remove data related to days or time for which the system worked improperly. This mainly consists in eliminating incomplete I-V curves or those recorded during strong variation of solar irradiance intensity. Then, the remaining curves (data without mishmash) are processed to extract three important electrical performances: the short circuit current (I_{sc}), the open circuit voltage (V_{oc}), and the maximum power (P_{mp}), as well as their corresponding voltage (V_{mp}) and current (I_{mp}).

- I_{sc} and V_{oc} are obtained by linear interpolation if the I-V curve intersects the reference axis and by linear extrapolation otherwise.
- P_{mp} is the most important parameter as the role of a PV system is to convert solar energy into electrical energy, and the efficiency of this process depends on the maximum power (P_{mp}). In order to determine the maximum power point, a set of points (V, P) is calculated, where P is the product of voltage V and current I. Then, a fourth-order polynomial least-square regression is applied to ten points around the point which corresponds to the maximum value of P (among the previous set of points). The point (V_{mp} , P_{mp}) of the maximum power corresponds to the maximum of the polynomial. The current I_{mp} is finally obtained by linear interpolation within the I-V curve points.

Finally, the extracted values of the maximum power are used to compute the performance ratio (PR) thanks to expression (4), which is derived from the expressions (1) to (3)

$$PR = \frac{P_{mp}}{P_{mp,stc}*S}, \quad (4)$$

where S is the number of suns expressing the solar irradiance level and defined as

$$S = \frac{G}{G_{STC}}. \quad (5)$$

Several studies ([Guérin de Montgareuil *et al.*, 2009](#) and [Merten *et al.*, 2008](#)) report that the use of a pyranometer to measure the incident irradiance (G) converted by the PV module regardless to its technology introduces errors in the performance ratio estimation and can lead to wrong

analysis. In fact, the pyranometers (Thermopile detector type) measure almost the total solar spectrum from 0.3 to 3 μm , while the spectral response of the PV module depends on its technology. In addition, the response time of the pyranometer is long and can reach 24 s. In this lap of time, the pyranometer is not sensitive to a solar irradiance variation. On the other hand, every 5 min, the bench successively measures the I-V curves of all the connected PV modules. Each I-V curve is measured in less than 2 s. Thus, it is often observed that the pyranometer displays, for several I-V curves, the same value of irradiance even though the latter varies due to many factors (solar spectrum, passing small clouds, etc.). For all these reasons and assuming a linear relation between the short circuit current I_{sc} and the irradiance G , many studies recommended (Guérin de Montgareuil *et al.*, 2009) the computation of the number of Suns with Eq. (6). The uncertainty relative to both the spectrum and the pyranometer response time is consequently reduced.

$$S = \frac{I_{sc}}{I_{sc,stc}}. \quad (6)$$

B. PR calculation from the electrical model

The approach used here is based on the one diode electrical model with five parameters (L5P) as shown in Fig. 2. This electrical model is described by the following equation:

$$I = I_{ph} - I_{0s} \left[\exp \left(\frac{q(V + R_s I)}{n N_{cell} kT} \right) - 1 \right] + \frac{V + R_s I}{R_{sh}}, \quad (7)$$

where V and I are the measured voltage and current, respectively, q the elementary charge, and N_{cell} the number of solar cells connected in series in the PV module. The five unknown parameters to be extracted from the I-V curve are I_{ph} the photocurrent, R_s the series resistance, R_{sh} the shunt resistance, n the ideality factor, and I_{0s} the reverse saturation current. The solar irradiance and temperature dependence all these parameters are detailed below.

The approach, detailed in a previous work (Tossa *et al.*, 2014), is implemented in the Simulink environment of Matlab to estimate outdoor performances of the PV module. Figure 3 shows the Simulink model designed for this purpose and composed by two blocks.

The first block (Meteo data) performs two specific tasks. First, it loads the weather data of the site (solar irradiance and ambient temperature) previously stored in an Excel file and converts them for an inclined plane of a given angle, based on the site geographical coordinates (latitude, longitude, and albedo). The site geographical coordinates are entered through a suitable Simulink dialog box. The converted weather data are then transferred to a second block representing both the PV module and the characterization bench (IV bench). The latter block uses the main equation (see formula 7) of the L5P model and the appropriate formulas (Tossa *et al.*, 2014) to extrapolate the electrical parameters from one reference weather condition to another. Let us mention that the dependence of the electrical parameters on temperature, and irradiance is still a matter of debate.

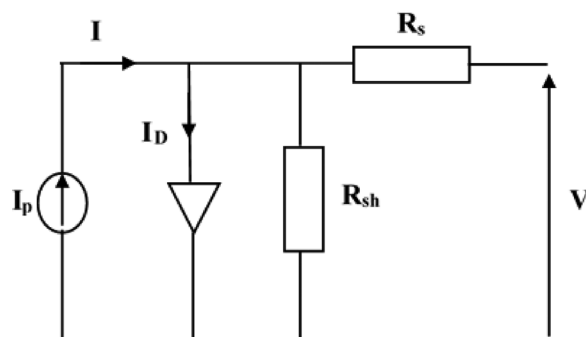


FIG. 2. Electrical model of the PV module with one diode and five parameters (L5P).

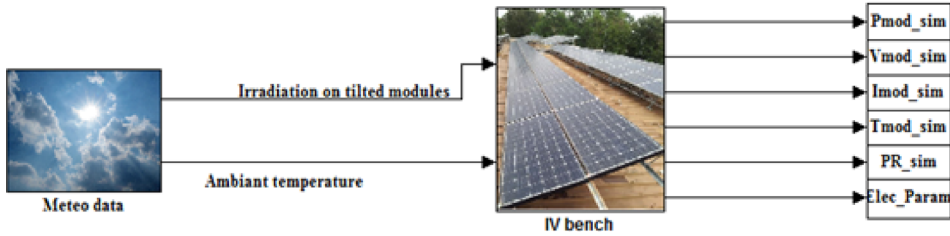


FIG. 3. Simulink model to estimate PV module performances under real operating conditions.

It is generally stated that the ideality factor and both the resistances R_s and R_{sh} are constant. However, some studies (Bai *et al.*, 2014; Chan *et al.*, 1986; De Blas *et al.*, 2002; De Soto *et al.*, 2006; and Ma *et al.*, 2014) observed the dependence of the parasitic resistances. In this study, only the ideality factor is considered constant, and the formulas for extrapolating the four remaining electrical parameters are given by the following equations which are widely used in the literature (Bai *et al.*, 2014; Ma *et al.*, 2014; and Tossa *et al.*, 2014).

$$I_{ph}(G, T) = I_{ph_{ref}} [1 + \alpha_{I_{SC}}(T - T_{ref})] \frac{G}{G_{ref}}, \quad (8)$$

$$I_0(T) = I_{0ref} \times \left(\frac{T}{T_{ref}} \right)^3 \times \exp \left(\frac{1}{k} \left(\frac{E_{g_{ref}}}{T_{ref}} - \frac{E_g(T)}{T} \right) \right), \quad (9)$$

$$E_g(T) = E_{g_{ref}} \cdot [1 - 0.0002677(T - T_{ref})], \quad (10)$$

$$R_s(G, T) = R_{S_{ref}} \cdot \left[\frac{T}{T_{ref}} \left(1 - \beta \times \ln \frac{G}{G_{ref}} \right) \right], \quad (11)$$

$$R_{sh}(G) = R_{sh_{ref}} \cdot \frac{G_{ref}}{G}. \quad (12)$$

The subscript “ref” refers to the parameters under a reference weather condition (G_{ref}, T_{ref}), T is the solar cell temperature, G the solar radiation, $\alpha_{I_{SC}}$ the temperature coefficient of the short-circuit current (available in the module data sheet), and β a coefficient whose value is approximately equal to 0.217 (Bai *et al.*, 2014). E_g is the semi-conductor material gap in eV. Its value is 1.12 eV for monocrystalline and multicrystalline (Avrutin *et al.*, 2014 and De Soto *et al.*, 2006) and 1.7 eV for amorphous and micromorph cells (Avrutin *et al.*, 2014 and Baroughi *et al.*, 2008). Thus, for each pair of solar irradiance and ambient temperature values, the IV bench block outputs the corresponding simulated I-V curve containing 100 points (V_{mod_sim} , I_{mod_sim}). The module maximal powers (P_{mod_sim}) are then extracted from the simulated I-V curves, according to the methodology described in Sec. III A. The PR of the module is finally computed thanks to Eqs. (4) and (6).

C. Design of the ANN model for the performance ratio calculation

1. Method of ANN model designing

Artificial Neural Networks (ANNs) are suitable for modeling complex real-world problems as they can learn from examples (measurements) and are able to deal with non-linear problems (Ceylan *et al.*, 2014a). They are composed of simple elements named neurons, operating in parallel and inspired by biological nervous systems (Demuth *et al.*, 2008). The ANN can be classified based on their architecture and the mathematical learning function they use. The two most widely used architecture (Basheer and Hajmeer, 2000) are Feed Forward Networks (FFNs) and Recurrent Networks (RNs). In a FFN, the data processing can extend over multiple (layers of)

units, but no feedback connections are present in contrast to RN used to model dynamic systems in which the state at a given time depends on the previous states. Thus, the FFN is mostly used to assess photovoltaic module performances ([Almonacid *et al.*, 2011](#); [Celik, 2011](#); [Ceylan *et al.*, 2014a, 2014b](#); [Mellit *et al.*, 2013](#); and [Velilla *et al.*, 2014](#)).

Among the three types of FFNs ([Gardner and Dorling, 1998](#)) (single-layer perceptron, multilayer perceptron, and radial basis function networks), the most used one is the multilayer perceptron (MLP).

A MLP basically consists of three layers of neurons: Input layer, Hidden layer, and Output layer as shown in Fig. 4. The number of input neurons is equal to the number of independent variables, while the output neuron(s) represent the dependent variable(s) (cf. Fig. 4). However, there is no magic rule ([Karsoliya, 2012](#)) to accurately determine the number of neurons in the hidden layer although this number plays a vital role in the ANN performances. If the number of neurons in the hidden layer is not enough, then “Underfitting” may occur ([Karsoliya, 2012](#)). On the other hand, more neurons than necessary in the network lead to “Overfitting.” Generally, the studies just report ([Celik, 2011](#); [Ceylan *et al.*, 2014b, 2014a](#); [Karamirad *et al.*, 2013](#); [Mellit *et al.*, 2013](#); and [Yap and Karri, 2015](#)) the number of neurons they use in the hidden layer without describing the process used to determine it. Some rule-of-thumb ([Karsoliya, 2012](#)) is usually used till now which does not provide the exact formula for calculating the number of hidden layer neurons.

The design of the ANN model requires the experimental data for the model training and its validation. The model training consists in modifying the ANN parameters so that the error between the model outputs and that of the actual system is sufficiently low. This fitting is done in this study, thanks to the well-known Levenberg-Marquardt algorithm. For the validation of the model, the network input data entered are different from those used for the training step. The output (i.e., the PR) should be equal or very close to the experimental values.

The method used here to determine the optimum number of neurons in the hidden layer of each module MLP model is based on the monitoring of the root mean-squared error (RMSE) obtained in both the training and validation phases. This method is recommended by [Basheer and Hajmeer \(2000\)](#) as the most appropriate one to find the optimum number of neurons in the hidden layer. Generally, the training error is a decreasing function of the number of neurons in the hidden layer, while the error in the validation phase shows an initial reduction and a subsequent increase due to memorization and overtraining of the ANN. The optimal number of neurons in the hidden layer is obtained at the onset of the increase in the error in the validation phase. For each module, the number of neurons is varied from 1 to 10. For each number of neurons in the hidden layer, ten trials (training and validation) are done and the corresponding

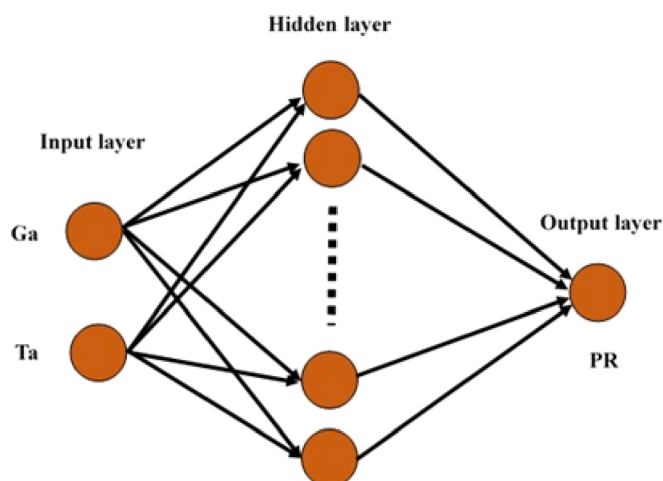


FIG. 4. Basic architecture of the MLP model.

root mean square error is computed. Then, only the network having the minimal value of RMSE in the validation phase is saved.

2. Method application

For this study, measurements recorded from April 1, 2015 to July 13, 2015 (about 3.5 months) by the I-V bench are considered. The training and validation data include solar irradiance in modules' plane, ambient temperature, and the performance ratio calculated with Eqs. (4) and (5). The dataset is then divided into two groups

- The first group of measurements from April 1, 2015 to April 29, 2015 (one month) is used to design the MLP model. 70% of the data are used for training and 30% for validation. Figure 5 shows the boxplot of the irradiance variation in the PV module plane during the first period (a) and the corresponding ambient temperatures (b).

During the observation period, the irradiance varied between 0 and 1017 W/m^2 , whereas the ambient temperature is between 21.89°C and 51.06°C . However, data of a few days or periods are missed (example, April 4, 2015 or April 14, 2015) due to external events, such as power cuts, general electrical blackouts, maintenance tasks, and disconnection of the sensors (Pt100, pyranometer). Here, the proportion of missing data is low enough so that the results are not affected.

- The second group of measurements from May 1, 2015 to July 13, 2015 (2.5 months) is used to test the MLP model and to compare its performances with those of the (L5P) electrical model.

Figures 6–9 present the determination of the optimum network for each PV module (a) and both the experimental and estimated PV module performance ratio curves in the network validation phase (b) for the selected optimum MLP.

From the recordings and Figs. 6–9, the following remarks can be made:

- When comparing Figs. 6 and 8, it is noted that the RMSE values in the validation phase can be either greater or lower than the values obtained in the training phase. This is due to the fact that the RMSE depends on the ANN inputs. In the present study, the recorded measurements are randomly divided into two groups, the first one (70% of the data) for training and the remaining data (30% of the data) for the validation;
- The optimal networks obtained for the selected PV modules have different numbers of neurons in their hidden layer. These numbers are 5, 5, 3, and 4 for the PV modules VIC003, VIC006, SUN011, and SHA017, respectively. This observation is quite coherent as the PV modules present different behavior regarding weather conditions. It may be particularly noted that the same number of neurons is obtained for both the PV modules VIC003 and VIC006, and furthermore, they present the same performance ratio on the site. Let us remind that these PV modules are not from the same technology (mono-Si and poly-Si) but are from the same manufacturer. It seems like there is no real difference between the performances of monocrystalline and polycrystalline PV modules from this manufacturer. This assumption can be consolidated when considering the technical data provided by the manufacturer (see Table I), and the STC characteristics of the two PV modules (VIC003 and VIC006) are almost equal.
- The micromorph PV module network yields a better value of RMSE although it has a lower number of neurons in the hidden layer (4 neurons) compared to 5 neurons for monocrystalline VIC003 and polycrystalline VIC006. Thus, the higher number of neurons in the hidden layer does not automatically mean a higher accuracy.
- The PV modules VIC006 and SUN011 have different numbers of neurons in their MLP models in the hidden layer although they belong to the same technology (polycrystalline). It seems like there is no clear relation between the PV module technologies and the number of neurons to be used in the hidden layer.
- The maximal number of neurons in the hidden layer is 5 for all the PV modules of this study, regardless of their technology. One can assume that 5 neurons in the hidden layer is sufficient to predict the performance ratio of silicon PV modules considered for this study.

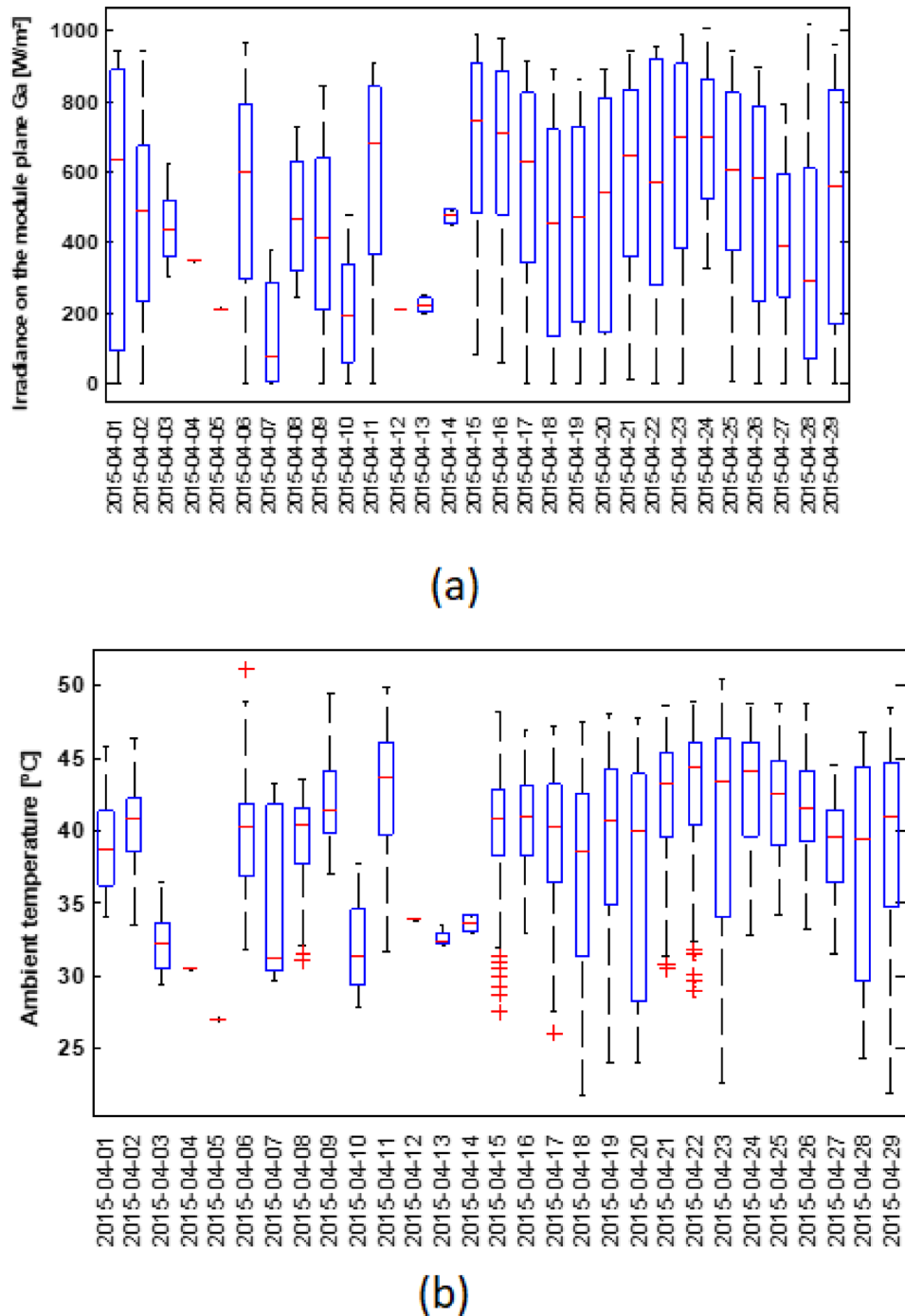


FIG. 5. Weather conditions as recorded from April 1, 2015 to April 29, 2015; (a) Irradiance on the PV module plane [W/m^2] and (b) Ambient temperature [$^{\circ}\text{C}$].

IV. RESULTS AND DISCUSSION

The reliability of the studied models (ANN versus L5P) was evaluated through two widely used parameters to estimate error: the root mean square error (RMSE) and the mean absolute percentage of error (MAPE). RMSE and MAPE are two statistical parameters defined by the following formulas:

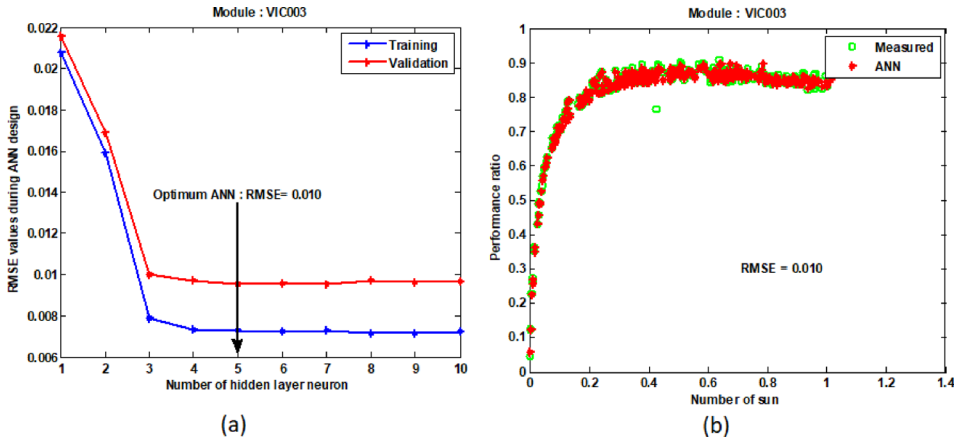


FIG. 6. (a) Selection of optimum MLP for VIC003. (b) Measured performance ratio and MLP model output in the validation phase.

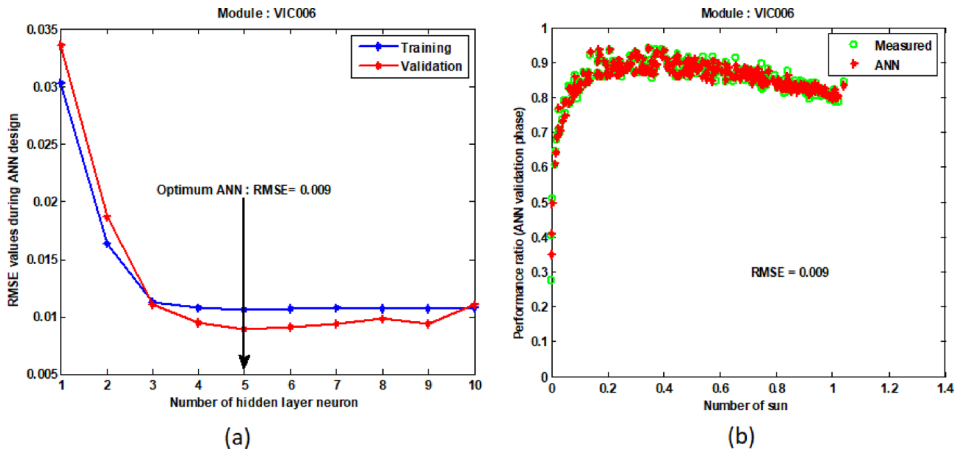


FIG. 7. (a) Selection of optimum MLP for VIC006. (b) Measured performance ratio and MLP model output in the validation phase.

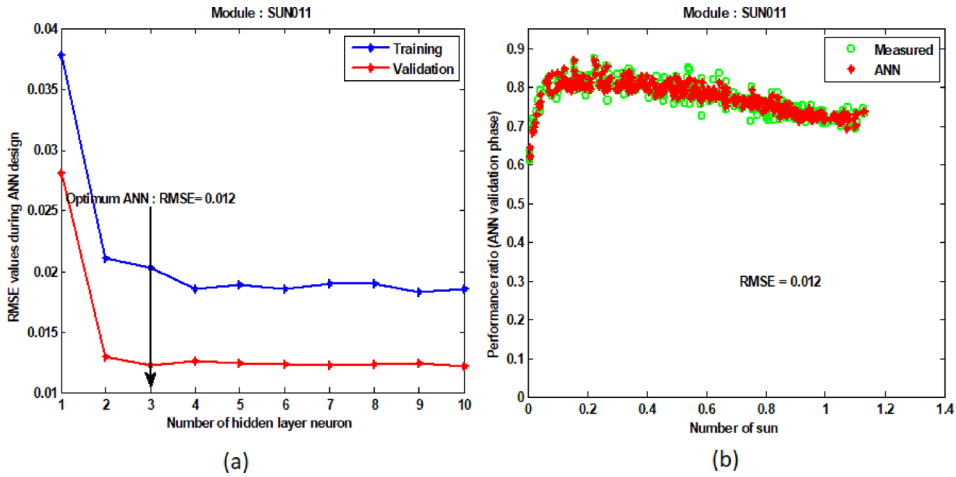


FIG. 8. (a) Selection of optimum MLP for SUN011. (b) Measured performance ratio and MLP model output in the validation phase.

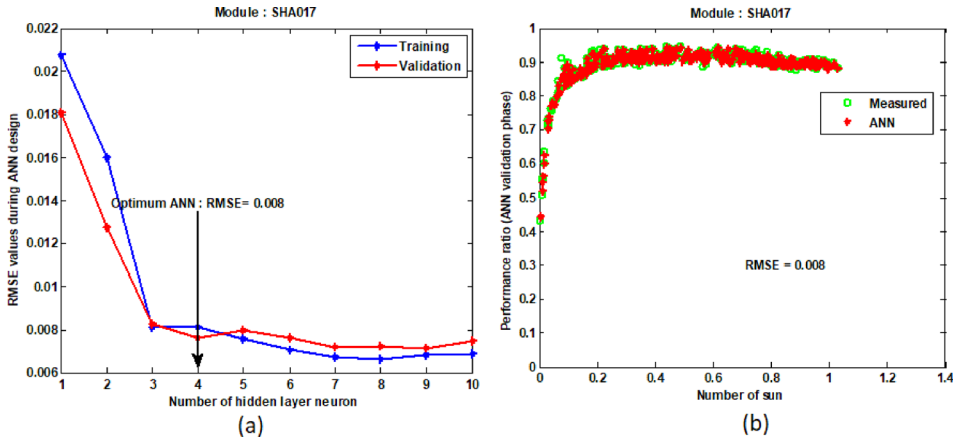


FIG. 9. (a) Selection of optimum MLP for SHA017. (b) Measured performance ratio and MLP model output in the validation phase.

$$RMSE = \sqrt{\left(\frac{1}{m}\right) \times \sum_{i=1}^m (PR_{modeli} - PR_{measi})^2}, \quad (13)$$

$$MAPE = \left(\frac{1}{m}\right) \times \sum_{i=1}^m \left| \frac{PR_{modeli} - PR_{measi}}{PR_{measi}} \right|, \quad (14)$$

where PR_{model} and PR_{meas} are the performance ratio calculated with the model and from experimental measurements, respectively.

A. Weather data

In order to test the designed MLP model, the dataset of the second period (from May 1, 2015 to July 13, 2015) is used as mentioned in Sec. III C. The values of ambient temperature used in this second period are deduced from PV module temperatures recorded in the same period. In fact, during this period, aberrant values of temperature were found within the ambient

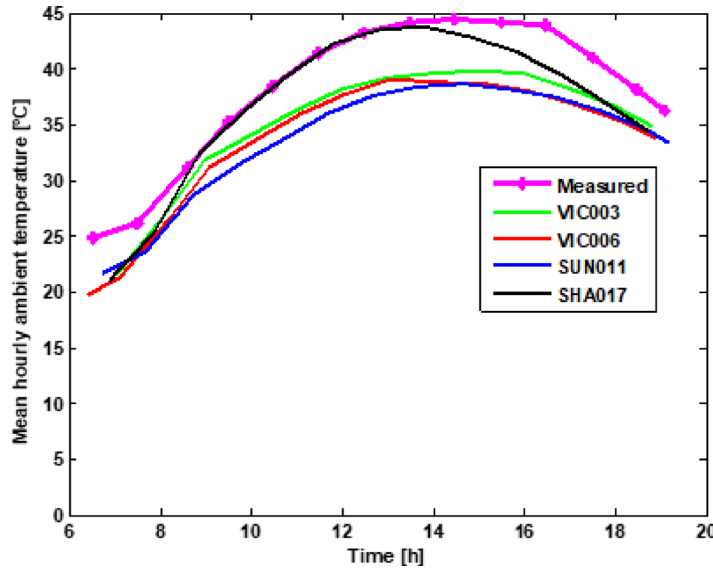


FIG. 10. Estimation of the hourly average of the site ambient temperature from the module temperature (from April 1, 2015 to April 29, 2015).

temperature values measured by the Pt100. It is well known ([Alonso García and Balenzategui, 2004](#); [Bai et al., 2014](#); [Ma et al., 2014](#)) that the PV module temperature can be easily estimated from solar irradiance and its NOCT value (Nominal Operation Cell Temperature) thanks to the following expression:

$$T_a = T_{mod} - \frac{G}{G_0} (T_{NOCT} - T_0). \quad (15)$$

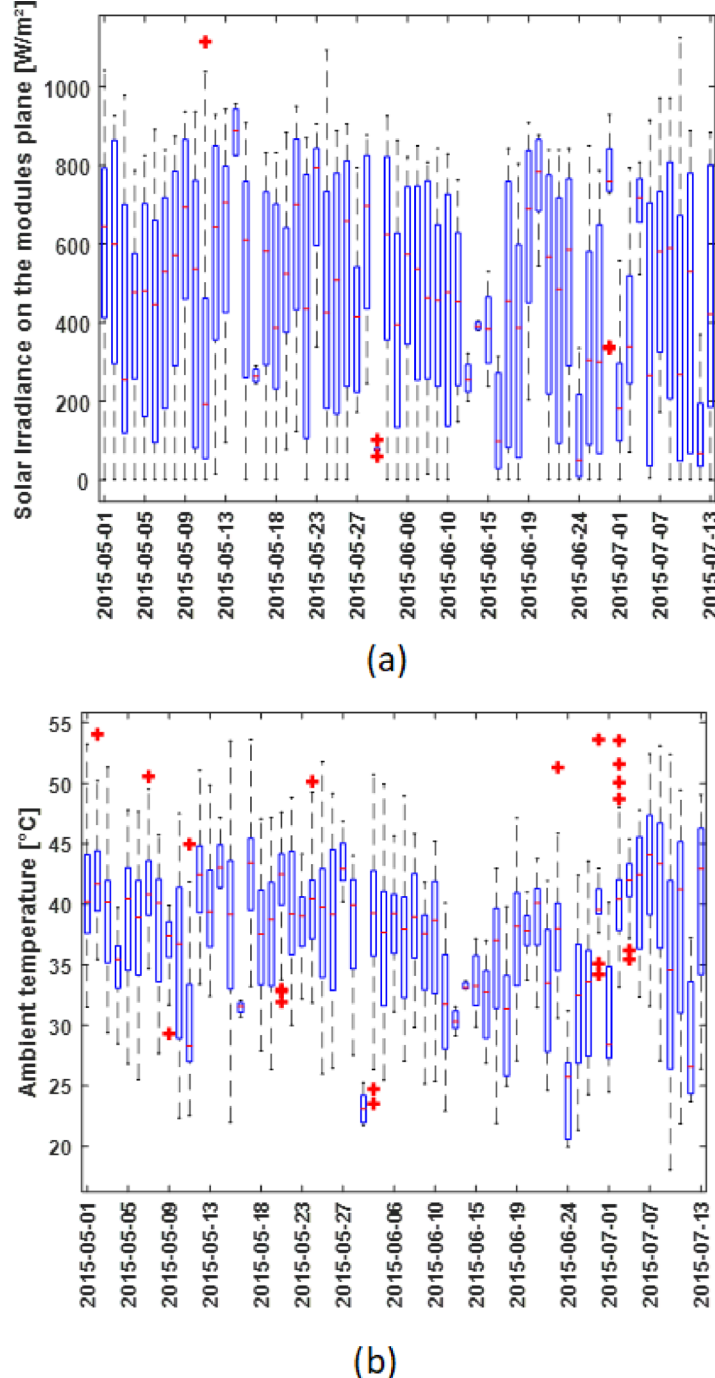


FIG. 11. Weather conditions as recorded from May 1, 2015 to July 13, 2015; (a) Irradiance on the module plane [W/m²] and (b) Ambient temperature [°C].

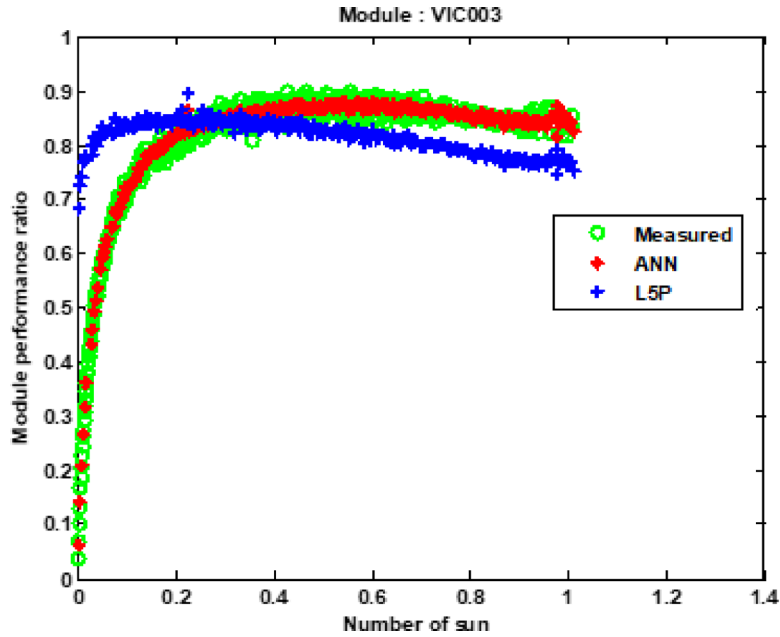


FIG. 12. Measured versus estimated performance ratios for different models (electrical L5P model, ANN) with respect to the number of suns for the module VIC003.

T_a and T_{mod} are the ambient and the module temperature in $^{\circ}\text{C}$; G [W/m^2] is the solar irradiance; T_{NOCT} is the cell temperature in NOCT conditions: a solar irradiance of $G_0 = 800 \text{ W}/\text{m}^2$ and an ambient temperature of $T_0 = 20^{\circ}\text{C}$.

In this study, expression (15) is modified by inserting a new parameter ε . This parameter takes into account the uncertainty in the cell nominal temperature (T_{NOCT}) measurement and the difference between the cell temperature and that of the back surface of the PV module

$$T_a = T_{mod} - \frac{G}{G_0} (T_{NOCT} - \varepsilon - T_0). \quad (16)$$

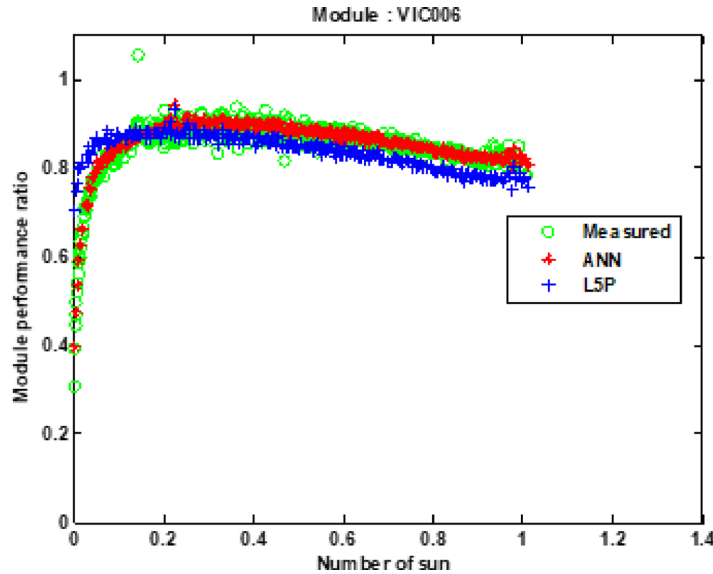


FIG. 13. Measured versus estimated performance ratios for different models (electrical L5P model, ANN) with respect to the number of suns for the PV module VIC006.

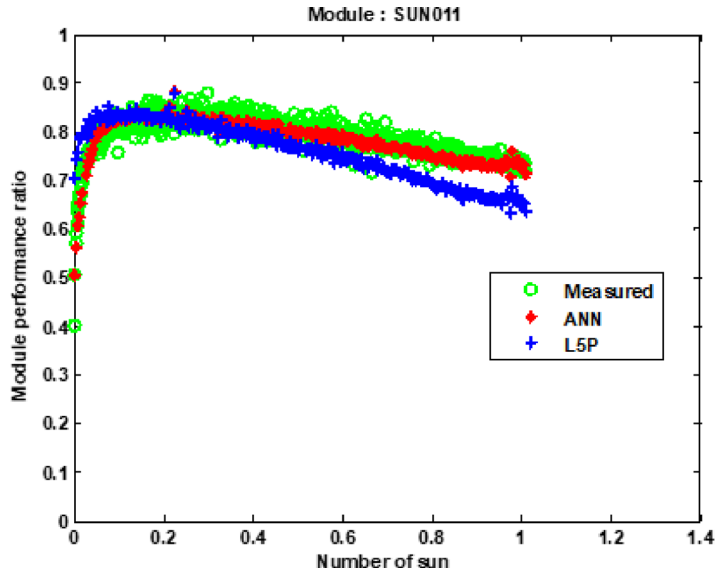


FIG. 14. Measured versus estimated performance ratios for different models (electrical L5P model, ANN) with respect to the number of suns for the PV module SUN011.

Before applying this model of module temperature, it will be carefully validated with the first measurements (data collected from April 1, 2015 to April 29, 2015) that have been correctly collected through the Pt100. It is found that the parameter ε varies from -3°C to 3°C . This range fits with the value of $\pm 3^{\circ}\text{C}$ widely used in the literature (Alonso García and Balenzategui, 2004 and Skoplaki and Palyvos, 2009). The optimal value of ε is the one which better fits the measured ambient temperatures by considering the root mean square error (RMSE) between the measured temperatures and the estimated values from module temperature. Figure 10 shows the hourly average values of the measured ambient temperatures and those estimated from the module temperatures. The optimum results are obtained with $\varepsilon = 3^{\circ}\text{C}$. The root mean square error (RMSE) values are 3.64°C , 4.5°C , 4.79°C , and 2.12°C for the modules VIC003, VIC006, SUN011, and SHA017, respectively. Even if these values

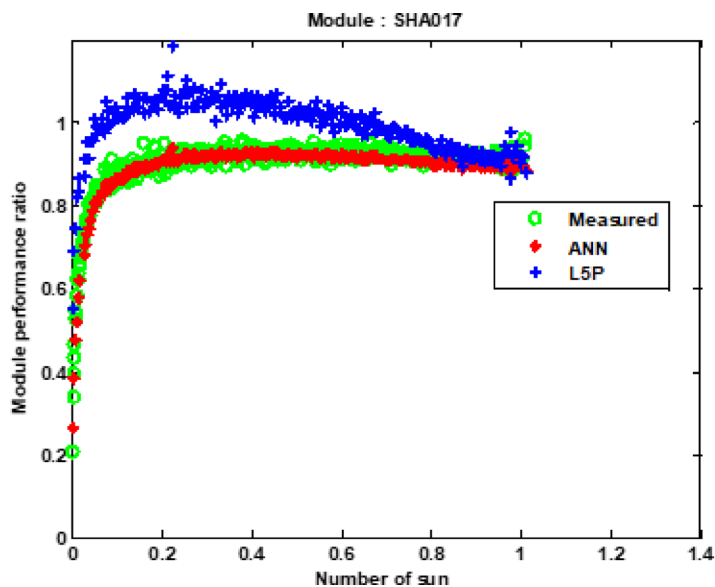


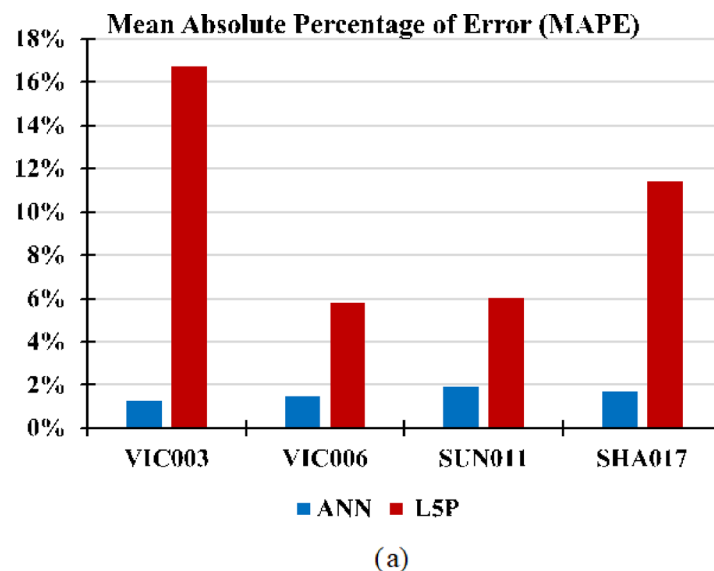
FIG. 15. Measured versus estimated performance ratios for different models (electrical L5P model, ANN) with respect to the number of suns for the PV module SHA017.

are relatively high, it may be noted that the best estimation is obtained with the micromorph module which also has the smallest RMSE. Moreover, the curve of micromorph (SHA017) correlates well with measurements in the sunniest time slot (9 am–2 pm).

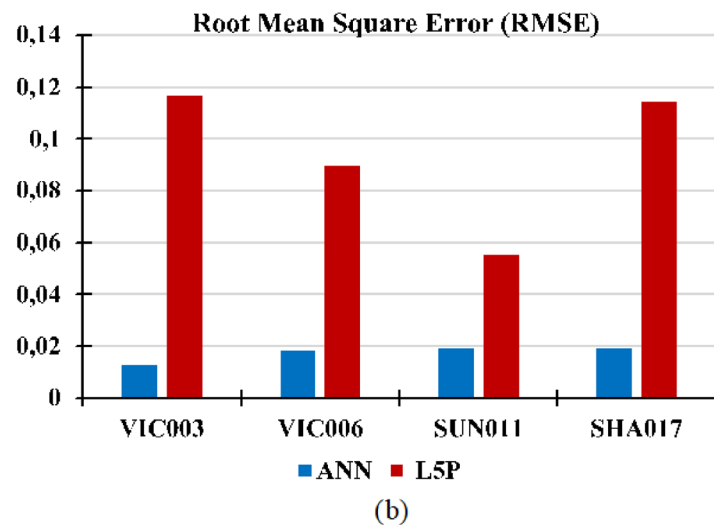
At last, the RMSE of the micromorph PV module (2.12°C) is consistent with the uncertainty of the nominal temperature measurement ($\pm 3^{\circ}\text{C}$). Therefore, the temperatures of the micromorph module were used to estimate the ambient temperature of the second dataset. Instead, irradiance is measured using a pyranometer during all the study as described in Sec. II. Figure 11(a) shows the irradiance in the module plane during the second period of data collection (from May 1, 2015 to July 13, 2015). The corresponding ambient temperatures deducted from the micromorph module temperatures are shown in Fig. 11(b).

B. ANN versus electrical model

Figures 12–15 depict the curves of the measured and estimated performance ratios of the studied PV modules from May 1, 2015 to July 13, 2015.



(a)



(b)

FIG. 16. (a) MAPE and (b) RMSE from the models (ANN and L5P) on the performance ratio estimated for the four studied PV modules.

Figure 16 shows the values of the two statistical errors expressed by Eqs. (13) and (14) for the four PV modules.

By referring to Figs. 12–16, the following key statements can be made:

- The ANN performance ratio curves are superimposed to those from the monitored values for all the PV modules. This means that ANN-based models estimate the profile of the performance ratio with high accuracy;
- The ANN-based models provide nearly the same values of RMSE for the PV modules. Regardless of the PV module type, the values remain lower than 0.02;
- The same observation can be made for the MAPE values which are also lower than 2% for the ANN based model, while these values vary from 6% to 17% for the L5P model;
- The L5P model predicted the PV module performance ratio with accuracy 3–9 times lower than that of neural networks (ANNs). That is consistent with the fact that the electrical model only

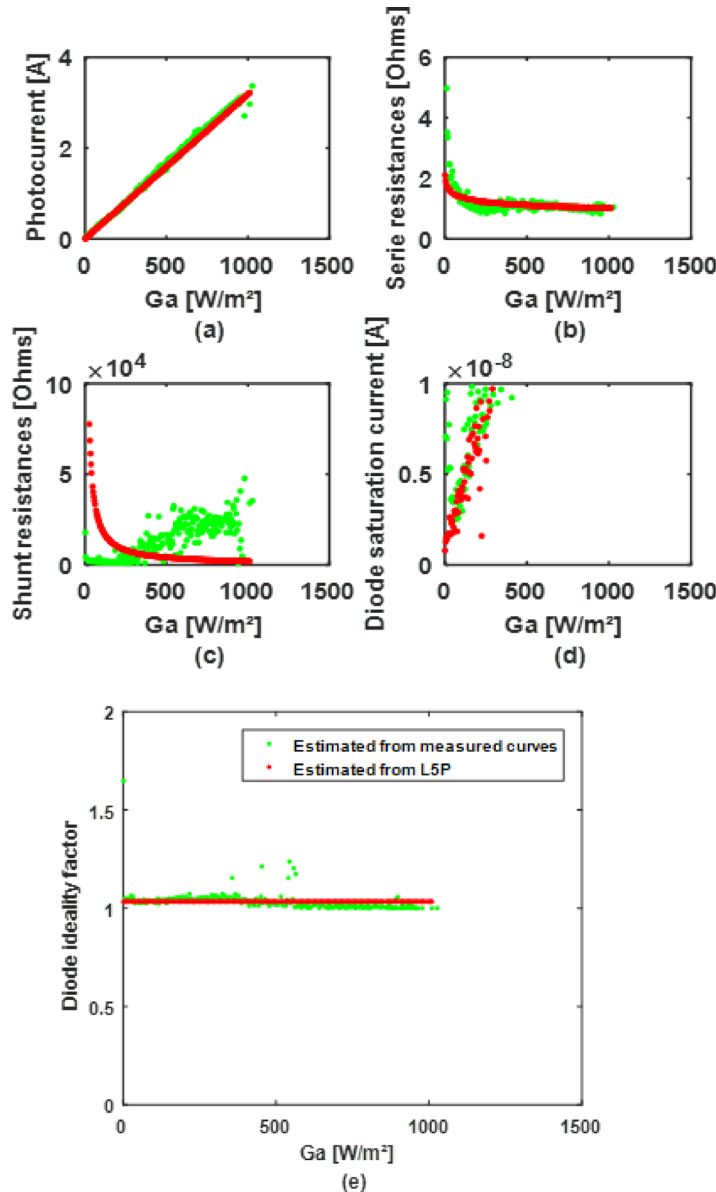


FIG. 17. Electrical parameters for polycrystalline module SUN011; comparison between the measured values and those calculated with the L5P model.

takes into account temperature losses, while the ANN-based model also takes in addition low irradiation losses, spectral and angular losses, and partially nominal power losses as reported by Almonacid *et al.* (2011);

- The L5P model seems to be more appropriate for polycrystalline PV modules (VIC006 and SUN011) than both monocrystalline (VIC003) and micromorph (SHA017) PV modules;
- The L5P model seems to underestimate the performance ratio of the crystalline technologies (VIC003, VIC006, and SUN011), in contrast to the micromorph PV module (SHA017).

Given the poor quality of the L5P model compared to the ANN one, the weaknesses of the LM approach (with the L5P model) are investigated. This will allow us not only to highlight some elements on which the LM approach can be improved but also to better understand the relatively poor performances of the LM approach when compared to ANN models. For this purpose, two modules are considered: polycrystalline and micromorph PV modules. The five electrical parameters of the L5P model were determined from I-V curves measured by the test facility as well as I-Vcurves estimated with the Simulink blocks. The extraction method is well

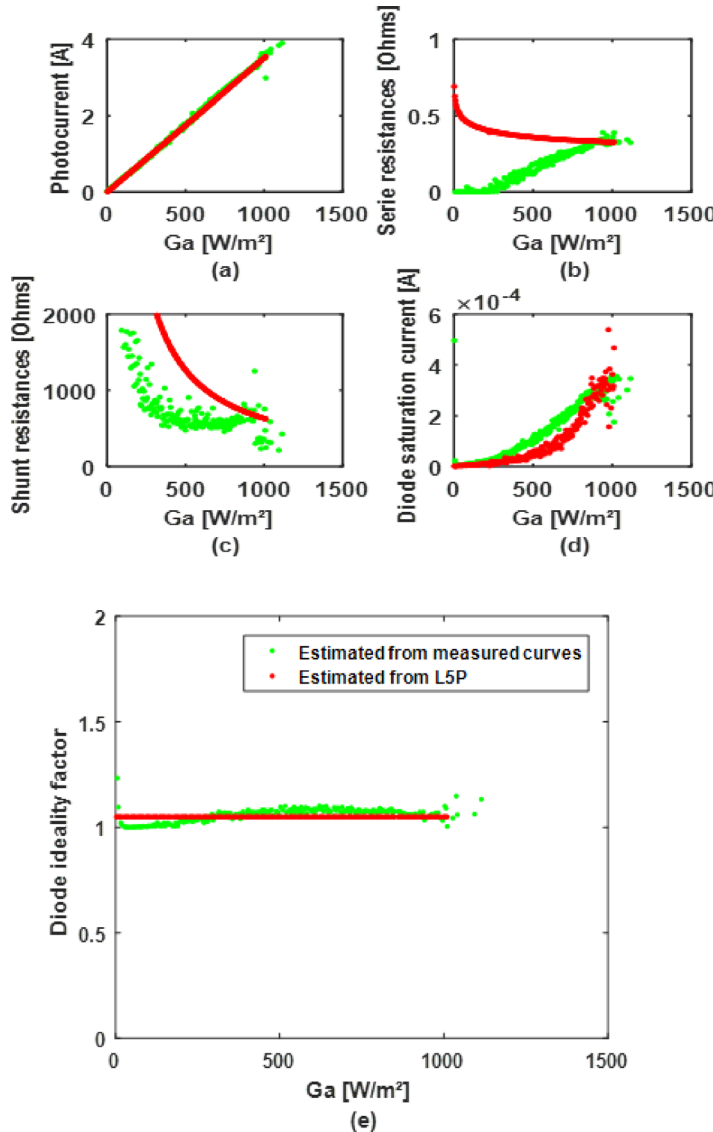


FIG. 18. Electrical parameters for micromorph module SHA017; comparison between measured values and those calculated with the L5P model.

described in a previous work (Tossa et al., 2014). Figures 17 and 18 depict the variation of five electrical parameters for each PV module.

From Figs. 17 and 18, one can observe that both the photocurrent and the diode parameters are well estimated. This confirms the accuracy of the well-known linear relationship [Eq. (3)] between the photocurrent and the irradiance. However, the parasite resistances (series and shunt) are poorly estimated. As a consequence, PV module performance ratios are overestimated. In fact, the series resistance greatly affects the PV module performance ratio under high values of irradiance (Merten et al., 2008 and van Dyk and Meyer, 2004), whereas the shunt resistance effect is noted for low values of irradiance (McMahon et al., 1996 and van Dyk and Meyer, 2004).

V. CONCLUSION

This paper deals with the modeling and the estimation of performance ratios of different photovoltaic module technologies under real operating conditions. Two different approaches have been presented. The first approach developed in the Matlab/Simulink environment is based on the one diode and five parameter electrical model (L5P). The second approach, also implemented in Matlab, is based on Artificial Neural Networks (ANNs), especially a multilayer perceptron (MLP) network. The two approaches were compared, through outdoor measurements from April 4, 2015 to July 13, 2015. The study focuses on four modules belonging to three different PV silicon technologies (one monocrystalline PV module, two polycrystalline PV modules, and one micromorph or tandem structure amorphous PV module). The measurements are performed thanks to the outdoor solar test facility set-up in Ouagadougou (Burkina Faso).

One part of the measurement is used to train and validate the MLP model on each PV module, while the second part is dedicated to the testing of the MLP models and to perform the comparison study. It has been shown that the number of neurons in the hidden layer is not a function of PV module technology and that a maximum value of 5 neurons is sufficient to estimate the performance ratios of silicon PV modules with good accuracy. The ANN models proposed in this work are able to estimate the module performance ratio for a real environment, with a root mean square error (RMSE) lower than 0.02 regardless of the module technology. Furthermore, this accuracy is 3–9 times better than that achieved with the approach based on the electrical model. On the other hand, the approach based on the electrical model works better for the polycrystalline technology than for monocrystalline and micromorph. Finally, in order to identify the weaknesses of the approach based on the L5P model, a focus was made on the variation of both measured and estimated electrical parameters regarding the site weather conditions. This analysis shows that the weaknesses of the L5P model fundamentally come from the wrong estimation of parasite series and shunt resistance.

- Almonacid, F., Pérez-Higueras, P. J., Fernández, E. F., and Hontoria, L., “A methodology based on dynamic artificial neural network for short-term forecasting of the power output of a PV generator,” *Energy Convers. Manage.* **85**, 389–398 (2014).
- Almonacid, F., Rus, C., Pérez-Higueras, P., and Hontoria, L., “Calculation of the energy provided by a PV generator. Comparative study: Conventional methods vs. artificial neural networks,” *Energy* **36**, 375–384 (2011).
- Alonso García, M. C. and Balenzategui, J. L., “Estimation of photovoltaic module yearly temperature and performance based on nominal operation cell temperature calculations,” *Renewable Energy* **29**, 1997–2010 (2004).
- Amrouche, B., Sicot, L., Guessoum, A., and Belhamel, M., “Experimental analysis of the maximum power point’s properties for four photovoltaic modules from different technologies: Monocrystalline and polycrystalline silicon, CIS and CdTe,” *Sol. Energy Mater. Sol. Cells* **118**, 124–134 (2013).
- Aste, N., Del Pero, C., and Leonforte, F., “PV technologies performance comparison in temperate climates,” *Sol. Energy* **109**, 1–10 (2014).
- Avrutin, V., Izyumskaya, N., and Morkoç, H., “Amorphous and micromorph Si solar cells: Current status and outlook,” *Turk. J. Phys.* **38**, 526–542 (2014).
- Bai, J., Liu, S., Hao, Y., Zhang, Z., Jiang, M., and Zhang, Y., “Development of a new compound method to extract the five parameters of PV modules,” *Energy Convers. Manage.* **79**, 294–303 (2014).
- Baroughi, M. F., Wang, J., and Shanmugam, M., “Micromorph Si-multicrystalline Si tandem solar cells for cost effective photovoltaics,” in *33rd IEEE Photovoltaic Specialists Conference, PVSC’08*, IEEE (2008), pp. 1–4.
- Basheer, I. A. and Hajmeer, M., “Artificial neural networks: Fundamentals, computing, design, and application,” *J. Microbiol. Methods* **43**, 3–31 (2000).

- Bonkoungou, D., Koalaga, Z., and Njomo, D., "Modelling and simulation of photovoltaic module considering single-diode equivalent circuit model in MATLAB," *Int. J. Emerg. Technol. Adv. Eng.* **3**, 493–502 (2013).
- Bücher, K., "Site dependence of the energy collection of PV modules," *Sol. Energy Mater. Sol. Cells* **47**, 85–94 (1997).
- Cañete, C., Carretero, J., and Sidrach-de-Cardona, M., "Energy performance of different photovoltaic module technologies under outdoor conditions," *Energy* **65**, 295–302 (2014).
- Celik, A. N., "Artificial neural network modelling and experimental verification of the operating current of monocrystalline photovoltaic modules," *Sol. Energy* **85**, 2507–2517 (2011).
- Ceylan, İ., Erkaymaz, O., Gedik, E., and Gürel, A. E., "The prediction of photovoltaic module temperature with artificial neural networks," *Case Stud. Therm. Eng.* **3**, 11–20 (2014a).
- Ceylan, İ., Gedik, E., Erkaymaz, O., and Gürel, A. E., "The artificial neural network model to estimate the photovoltaic modul efficiency for all regions of the Turkey," *Energy Build.* **84**, 258–267 (2014b).
- Chan, D. S. H., Phillips, J. R., and Phang, J. C. H., "A comparative study of extraction methods for solar cell model parameters," *Solid-State Electron.* **29**, 329–337 (1986).
- Cornaro, C. and Musella, D., "Performance analysis of PV modules of various technologies after more than one year of outdoor exposure in Rome," in Proceedings of the III International Conference on Applied Energy (2011).
- De Blas, M. A., Torres, J. L., Prieto, E., and García, A., "Selecting a suitable model for characterizing photovoltaic devices," *Renewable Energy* **25**, 371–380 (2002).
- De Soto, W., Klein, S. A., and Beckman, W. A., "Improvement and validation of a model for photovoltaic array performance," *Sol. Energy* **80**, 78–88 (2006).
- Demuth, H., Beale, M., and Hagan, M., *Neural Network ToolboxTM 6 User's guide*. Mathworks Inc. (2008).
- Gardner, M. W. and Dorling, S. R., "Artificial neural networks (the multilayer perceptron)—a review of applications in the atmospheric sciences," *Atmos. Environ.* **32**, 2627–2636 (1998).
- Guérin de Montgareuil, A., Sicot, L., Martin, J.-L., Mezzasalma, F., Delesse, Y., and Merten, J., "A new tool for the MotherPV method: Modeling of the Irradiance Coefficient of Photovoltaic Modules," in *24th European Photovoltaic Solar Energy Conference*, 21–25 September 2009, Hamburg, Germany (2009), pp. 3305–3309.
- Guérin de Montgareuil, A., Sicot, L., Mohring, H., Stellbogen, D., Zdanowicz, T., Prorok, M., Kolodenny, W., Martin, J.-L., Mezzasalma, F., Delesse, Y., and Merten, J., "First results of the application of the MotherPV method to CIS modules," in *24th European Photovoltaic Solar Energy Conference*, 21–25 September 2009, Hamburg, Germany (2009), pp. 3451–3455.
- Kamkird, P., Ketjoy, N., Rakwichian, W., and Sukchai, S., "Investigation on temperature coefficients of three types photovoltaic module technologies under Thailand operating condition," *Procedia Eng.* **32**, 376–383 (2012).
- Karamirad, M., Omid, M., Alimardani, R., Mousazadeh, H., and Heidari, S. N., "ANN based simulation and experimental verification of analytical four- and five-parameters models of PV modules," *Simul. Model. Pract. Theory* **34**, 86–98 (2013).
- Karsoliya, S., "Approximating number of hidden layer neurons in multiple hidden layer BPNN architecture," *Int. J. Eng. Trends Technol.* **3**, 713–717 (2012).
- Kurnik, J., Jankovec, M., Brecl, K., and Topic, M., "Outdoor testing of PV module temperature and performance under different mounting and operational conditions," *Sol. Energy Mater. Sol. Cells* **95**, 373–376 (2011).
- Ma, T., Yang, H., and Lu, L., "Development of a model to simulate the performance characteristics of crystalline silicon photovoltaic modules/strings/arrays," *Sol. Energy* **100**, 31–41 (2014).
- Makrides, G., Zinsser, B., Georgiou, G. E., Schubert, M., and Werner, J. H., "Temperature behaviour of different photovoltaic systems installed in Cyprus and Germany," *Sol. Energy Mater. Sol. Cells* **93**, 1095–1099 (2009).
- Makrides, G., Zinsser, B., Georgiou, G. E., Schubert, M., and Werner, J. H., "Outdoor efficiency of different photovoltaic systems installed in Cyprus and Germany," in *33rd IEEE Photovoltaic Specialists Conference, 2008. PVSC'08*, IEEE (2008), pp. 1–6.
- McMahon, T. J., Basso, T. S., and Rummel, S. R., "Cell shunt resistance and photovoltaic module performance," in *Conference Record of the Twenty Fifth IEEE Photovoltaic Specialists Conference, 1996*, IEEE (1996), pp. 1291–1294.
- Mellit, A., Sağlam, S., and Kalogirou, S. A., "Artificial neural network-based model for estimating the produced power of a photovoltaic module," *Renewable Energy* **60**, 71–78 (2013).
- Merten, J., Sicot, L., Delesse, Y., and de Montgareuil, A. G., "Outdoor evaluation of the energy production of different module technologies," in *Proceeding of the 23rd European Photovoltaic Solar Energy Conference Exhibition* (2008), pp. 2841–2845.
- Merten, J., Sicot, L., Delesse, Y., Martin, J.-L., Mezzasalma, F., and Guérin de Montgareuil, A., "In situ monitoring of degradation processes inside PV modules of different technologies," in *24th European Photovoltaic Solar Energy Conference*, 21–25 September 2009, Hamburg, Germany (2009), pp. 3490–3493.
- Merten, J., Sicot, L., Delesse, Y., and Montgareuil, A. G., "Outdoor evaluation of the energy production of different module technologies," in *Proceedings of the 22nd European Photovoltaic Solar Energy Conference*, Eds2008 (2008).
- Mosalam Shaltout, M. A., El-Hadad, A. A., Fadly, M. A., Hassan, A. F., and Mahrous, A. M., "Determination of suitable types of solar cells for optimal outdoor performance in desert climate," *Renewable Energy* **19**, 71–74 (2000).
- Ndiaye, A., Kébé, C. M. F., Charki, A., Ndiaye, P. A., Sambou, V., and Kobi, A., "Degradation evaluation of crystalline-silicon photovoltaic modules after a few operation years in a tropical environment," *Sol. Energy* **103**, 70–77 (2014).
- Phinikarides, A., Kindyni, N., Makrides, G., and Georgiou, G. E., "Review of photovoltaic degradation rate methodologies," *Renewable Sustainable Energy Rev.* **40**, 143–152 (2014).
- Piliougine, M., Carretero, J., Mora-López, L., and Sidrach-de-Cardona, M., "Experimental system for current-voltage curve measurement of photovoltaic modules under outdoor conditions," *Prog. Photovoltaics Res. Appl.* **19**, 591–602 (2011).
- Rüther, R., Kleiss, G., and Reiche, K., "Spectral effects on amorphous silicon solar module fill factors," *Sol. Energy Mater. Sol. Cells* **71**, 375–385 (2002).
- Sharma, V., Kumar, A., Sastry, O. S., and Chandel, S. S., "Performance assessment of different solar photovoltaic technologies under similar outdoor conditions," *Energy* **58**, 511–518 (2013).
- Sicot, L., Razongles, G., Merten, J., Mezzasalma, F., Martin, J.-L., Favre, W., Delesse, Y., and Guérin de Montgareuil, A., "From watt-peak to watt-hours: MotherPV method and IEC 61853 standard," in *28th European Photovoltaic Solar Energy Conference Exhibition* (2013), pp. 2935–2938.

- Skoplaki, E. and Palyvos, J. A., “On the temperature dependence of photovoltaic module electrical performance: A review of efficiency/power correlations,” *Sol. Energy* **83**, 614–624 (2009).
- Tossa, A. K., Soro, Y. M., Azoumah, Y., and Yamegueu, D., “A new approach to estimate the performance and energy productivity of photovoltaic modules in real operating conditions,” *Sol. Energy* **110**, 543–560 (2014).
- Tossa, A. K., Soro, Y. M., Thiaw, L., Azoumah, Y., Sicot, L., Yamegueu, D., Lishou, C., Coulibaly, Y., and Razongles, G., “Energy performance of different silicon photovoltaic technologies under hot and harsh climate,” *Energy*, **103**, 261–270 (2016).
- Van Dyk, E. E. and Meyer, E. L., “Analysis of the effect of parasitic resistances on the performance of photovoltaic modules,” *Renewable Energy* **29**, 333–344 (2004).
- Velilla, E., Valencia, J., and Jaramillo, F., “Performance evaluation of two solar photovoltaic technologies under atmospheric exposure using artificial neural network models,” *Sol. Energy* **107**, 260–271 (2014).
- World Nuclear Association, <http://www.world-nuclear.org/information-library/energy-and-the-environment/renewable-energy-and-electricity.aspx> for “Renewable Energy and Electricity” (accessed 3.2.2017).
- Yap, W. K. and Karri, V., “An off-grid hybrid PV/diesel model as a planning and design tool, incorporating dynamic and ANN modelling techniques,” *Renewable Energy* **78**, 42–50 (2015).